Combined treatment with bortezomib plus bafilomycin A_1 enhances the cytocidal effect and induces endoplasmic reticulum stress in U266 myeloma cells: Crosstalk among proteasome, autophagy-lysosome and ER stress

TOMOHIRO KAWAGUCHI[1*], KEISUKE MIYAZAWA[1*], SHOTA MORIYA[1], TADASHI OHTOMO[1], XIAO-FANG CHE[1], MUNEKAZU NAITO[2], MASAHIRO ITOH[2] and AKIO TOMODA[1]

Departments of [1]Biochemistry and [2]Anatomy, Tokyo Medical University, Tokyo, Japan

Received October 4, 2010; Accepted December 1, 2010

DOI: 10.3892/ijo.2010.882

Abstract. Bortezomib (BZ), a first line 26S proteasome inhibitor, induces a potent cytocidal effect with caspase-3 activation in multiple myeloma (MM) cell lines. Since IκBα is a substrate of the proteasome, the initial rationale for using BZ in MM has been to inhibit NF-κB. However, BZ rather activated NF-κB activity in U266 cells. BZ induces autophagy as well as endoplasmic reticulum (ER) stress in various cell lines tested. Inhibition of initial autophagosome formation by treatment with either 3-methyladenine or siRNA for LC3B in U266 cells and knockdown of the atg5 gene in a murine embryonic fibroblastic cell line all resulted in attenuation of BZ-induced cell death. In contrast, combined treatment with BZ and bafilomycin A_1 (BAF), which is a specific inhibitor of vacuolar-ATPase and is used as an autophagy inhibitor at the late stage, resulted in synergistic cytotoxicity, compared with that by either BZ or BAF alone. BAF treatment also induced ER stress, but the kinetics of inductions of ER stress-related genes [e.g. CHOP (GADD153) and GRP78] completely differed between BZ- and BAF-treatments: BZ induced these ER stress markers within 8 h, whereas treatment with BAF required more than 48 h in U266 cells. In order to synchronize ER stress, we pre-treated U266 cells with BAF for 48 h, followed with BZ for 48 h. The sequential treatment with BAF and BZ induced a further enhanced cytotoxicity, compared with the simultaneous combination of BAF and BZ. These data suggest crosstalk among the ubiquitin-proteasome system, the autophagy-lysosome system, and ER stress. Controlling these interactions and kinetics appears to have important implications for optimizing clinical cancer treatment including MM-therapy.

Correspondence to: Dr Keisuke Miyazawa, Department of Biochemistry, Tokyo Medical University, 6-1-1, Shinjuku, Shinjuku-ku, Tokyo 160-8402, Japan
E-mail: miyazawa@tokyo-med.ac.jp

*Contributed equally

Key words: bortezomib, autophagy, myeloma, apoptosis, ER stress

Introduction

Multiple myeloma (MM) is an incurable plasma cell neoplasia characterized by the production of large amounts of monoclonal immunoglobulins. Bortezomib (Velcade: BZ) is the first proteasome inhibitor to be approved for treatment of relapsed multiple myeloma (1-4). The promising anti-cancer activity by BZ in MM and other malignant cells has further proved that the proteasome is a legitimate target in cancer treatment (1,3). It is well known that constitutive nuclear factor (NF)-κB activity in MM cells mediates survival as well as resistance to chemotherapy and radiotherapy, by inducing the expression of anti-apoptotic proteins, adhesion molecules, and autocrine growth factors such as interleukin-6 (1,4). Since IκBα is a substrate of the proteasome, the initial rationale for using BZ in MM was to inhibit NF-κB (5,6).

Recent reports demonstrated that endoplasmic reticulum (ER) stress in response to BZ is another molecular-based mechanism for BZ-induced cytotoxicity in MM cells and other cancer cells (7,8). ER is an organelle found in eukaryotic cells for key functions, such as calcium sequestration, protein translation, folding and maturation. However, ER also has an important role as a sensor for cellular stress: it detects changes in cell homeostasis and responds by triggering signal transduction pathways, known as unfolded protein response (UPR) (9). Proteins that fail to adopt the correct conformation are retrotranslocated to the cytosol, and they are ubiquitinated and degraded by the 26S proteasome through ER-associated degradation (ERAD). When the amount of unfolded protein exceeds the capacity of the system, the proteins begin to aggregate in the ER, triggering a programmed death pathway, usually via apoptosis by induction of proapoptotic proteins such as CHOP (GADD153) (9,10). Therefore, proteasome inhibition appears to prevent the clearance of unfolded proteins through the ERAD system, which may result in ER stress-mediated apoptosis. One of the specific biological characteristics of MM is monoclonal immunoglobulin production.

Table I. Sequence of primers and annealing conditions for real-time PCR.

Symbol	Accession no.	Forward (5'-3')	Reverse (5'-3')	Annealing temp (°C)	Product size (bp)
ATF6	NM_007348.2	AAGCCCTGATGGTGCTAACTGAA	CATGTCTATGAACCCATCCTCGAA	60	126
PERK	NM_004836.4	GCTTATGCCAGACACACAGGACA	CTCCATCTGAGTGCTGAATGGATAC	60	150
IRE1	NM_001433.3	CCCGATCGTGAAGCAGTTAGA	CAGAACCACCTTTATAGGTCCTGAA	60	122
GRP78	NM_005347.3	CCTAGCTGTGTCAGAATCTCCATCC	GTTTCAATGTCACCATCCAAGATCC	60	80
ATF4	NM_182810.1	CTGCCCGTCCCAAACCTTAC	GCCCTCTTCTTCTGGCGGTA	60	139
CHOP	NM_004083.4	AAATCAGAGCTGGAACCTGAGGA	CCATCTCTGCAGTTGGATCAGTC	60	112
GADD34	NM_014330.3	AACCAGCAGTTCCCTTCCTG	TTGCCTCTCGCTCACCATAC	60	74
BIM	NM_207002.2	CATCATCGCGGTATTCGGTTC	AAGGTTGCTTTGCCATTTGGTC	60	141
BCL-2	NM_000633.2	TCAGCATGGCTCAAAGTGCAG	GAAACAGATGTCCCTACCAACCAGA	60	151
GAPDH	NM_002046.3	GCACCGTCAAGGCTGAGAAC	TGGTGAAGACGCCAGTGGA	60	138

Using IgG-secreting human MM cell line JK-6 and murine μH-chain transfected Ag8.H myeloma cells, proteasome inhibitors induce apoptosis preferentially in cells with a high synthesis rate of immunoglobulin associated with the accumulation of unfolded protein in ER (7). These data appear to explain the preferential therapeutic effect of BZ in MM, compared with other types of cancer, and suggest that ER-mediated apoptosis is involved in the cytotoxic effect of BZ in MM cells (7,8).

Besides the ubiquitin-proteasome system, autophagy is another intracellular degradation system that delivers cytoplasmic constitutions to the lysosome. Intracellular proteins and organelles including ER are engulfed in double-membrane vesicles called autophagosomes. The autophagosomes and lysosomes subsequently fuse to form autolysosomes in which the cargo of the autophagosome is degraded by lysosomal hydrolases (11,12). Autophagy is a process by which cells can adapt their metabolism to starvation nutrients or is a typical consequence of loss of growth factor signals, allowing cells to evade programmed cell death. However, in addition to its role in the starvation process, accumulating evidence suggests that autophagy is closely related to intracellular quality control of proteins and organelles, immune response, tumor suppression, anti-aging, and cell death (11,12). Recent reports demonstrated the selective degradation pathway of ubiquitinated protein through autophagy via p62 and related protein NBR1, which are docking proteins having both a microtubule-associated protein 1 light chain 3 (LC3)-interacting region and a ubiquitin-associated (UBA) domain. LC3 is essential for autophagy and is associated with autophagosome membranes after processing. Therefore, by binding ubiquitin via their C-terminal UBA domains, p62-mediated degradation of ubiquitinated cargo occurs by selective autophagy. Thus, the two intracellular degradation systems are directly linked (13-15). Additionally, ER-stress inducers (e.g., thapsigargin and tunicamycin) induce autophagy, indicating the connection of UPR to autophagy (16,17).

The previous data suggest linkage among the ubiquitin-proteasome system, the autophagy-lysosome system, and ER stress (10,18). Therefore, it is highly speculated that simultaneous inhibition of both degradation system may enhance ER stress-medicated apoptosis. We investigated the optimal conditions for inducing cell death in MM cell lines.

Materials and methods

Cell lines and reagents. For this study, U266 and IM-9 (MM cell lines), HL-60 and U937 [acute myeloid leukemia (AML) cell lines], A549 (a lung cancer cell line), and COLO201 (a colon cancer cell line) were obtained from the American Type Culture Collection (Rockville, MD) and were maintained in continuous culture in RPMI-1640 medium (Gibco, Grand Island, NY) supplemented with 10% FBS (Gibco), 2 mM L-glutamine, penicillin (50 U/ml), and streptomycin (100 μg/ml) (Gibco) in a humidified incubator containing 5% CO_2 and 95% air at 37˚C.

BZ was purchased from Toronto Research Chemicals Inc. (North York, Ontario, Canada), bafilomycin A_1 and tunicamycin were purchased from Sigma-Aldrich (St. Louis, MO), 3-methyladenine (3-MA) was purchased from MP Biomedicals (Solon, OH), and MG-132 was purchased from Calbiochem (Darmstadt, Germany).

Assessment of viable cell number and morphology in cultured cells. The viable cell number was assessed by CellTiter Blue, a cell viability assay kit (Promega Co., Madison, WI), with fluorescence measurements at 570 nm for excitation and 590 nm for fluorescence emission. For morphologic assessment, the cell suspensions were sedimented and fixed on slide glasses using a Shandon Cytospin II (Shandon, Pittsburgh, PA). Preparations were then stained with May-Grünwald-Giemsa, and examined using a degital microscope BZ-9000 (Keyence Co., Osaka, Japan).

Immunoblotting. Immunoblotting was performed as previously described (19). In short, cells were lysed with RIPA Lysis Buffer (Santa Cruz Biotechnology Inc., Santa Cruz, CA) containing 1 mM PMSF, 0.15 U/ml aprotinin, 10 mM EDTA, 10 mg/ml sodium fluoride, and 2 mM sodium orthovanadate. Cellular proteins were quantified using a DC Protein Assay kit of Bio-Rad (Richmond, CA). Equal amounts of proteins were loaded onto the gels, separated by SDS-PAGE and trans-

ferred onto Immobilone-P membrane (Millipore Corp., Bedford, MA). The membranes were probed with first antibodies (Abs) such as anti-microtubule-associated protein 1 light chain 3 (LC3) B Ab (Novus Biologicals, Inc., Littleton, CO), anti-Atg5 Ab (Cosmo Bio Co., Ltd., Tokyo, Japan), anti-cleaved caspase-3 (Asp175) Ab, anti-phospho-JNK (Thr183/Tyr185) Ab, and anti-phospho-eIF2α (Ser51) Ab, (Cell Signaling Technology, Danvers, MA), and anti-p62 (sequestosome-1) mAb, anti-CHOP (GADD153) Ab, anti-GAPDH mAb, and anti-ß-actin mAb (Santa Cruz). Immunoreactive proteins were detected with horseradish peroxidase-conjugated second Abs and an enhanced chemiluminescence reagent (ECL) (Millipore). Densitometry was performed using a Molecular Imager, ChemiDoc XRS system (Bio-Rad).

Electron microscopy. Cells were treated with or without BZ, and fixed with a solution containing 3% glutaraldehyde plus 2% paraformaldehyde in 0.1 M cacodylate buffer (pH 7.3) for 1 h. The samples were further post-fixed in 1% OsO_4 in the same buffer for 1 h, and subjected to electron microscopic analysis using an electron microscope H-7000 (Hitachi, Tokyo, Japan) as described previously (19).

Subcellular localization of NF-κB and IκBα. Subcellular localization of NF-κB/IκBα as well as the phosphorylation state of IκBα was assessed as previously described (20). After treatment with/without BZ, cells were harvested and lysed in 0.6% NP-40 Lysis Buffer A, which contained 10 mM HEPES (pH 7.9), 10 mM KCL, 0.2 mM EDTA, 1 mM dithiothreitol, 0.5 mM p-(amidinophenyl)methanesulfonyl fluoride (p-APMSF), for 30 min. The lysates were centrifuged at 250 x g for 10 min. The supernatant was then collected as the cytoplasmic fraction. The pellets containing the nuclei were washed in Buffer A without NP-40 and re-suspended in 50 μl of Nuclear Lysis Buffer containing 20 mM HEPES (pH 7.9), 0.4 M NaCl, 2 mM EDTA, 1 mM dithiothreitol and 1 mM PMSF, incubated for 30 min at 4˚C, and centrifuged at 20,000 x g for 20 min. The supernatants were used as nuclear fraction. Lysates containing 100 μg protein were subjected to SDS-PAGE and then transferred to an Immobilon-P

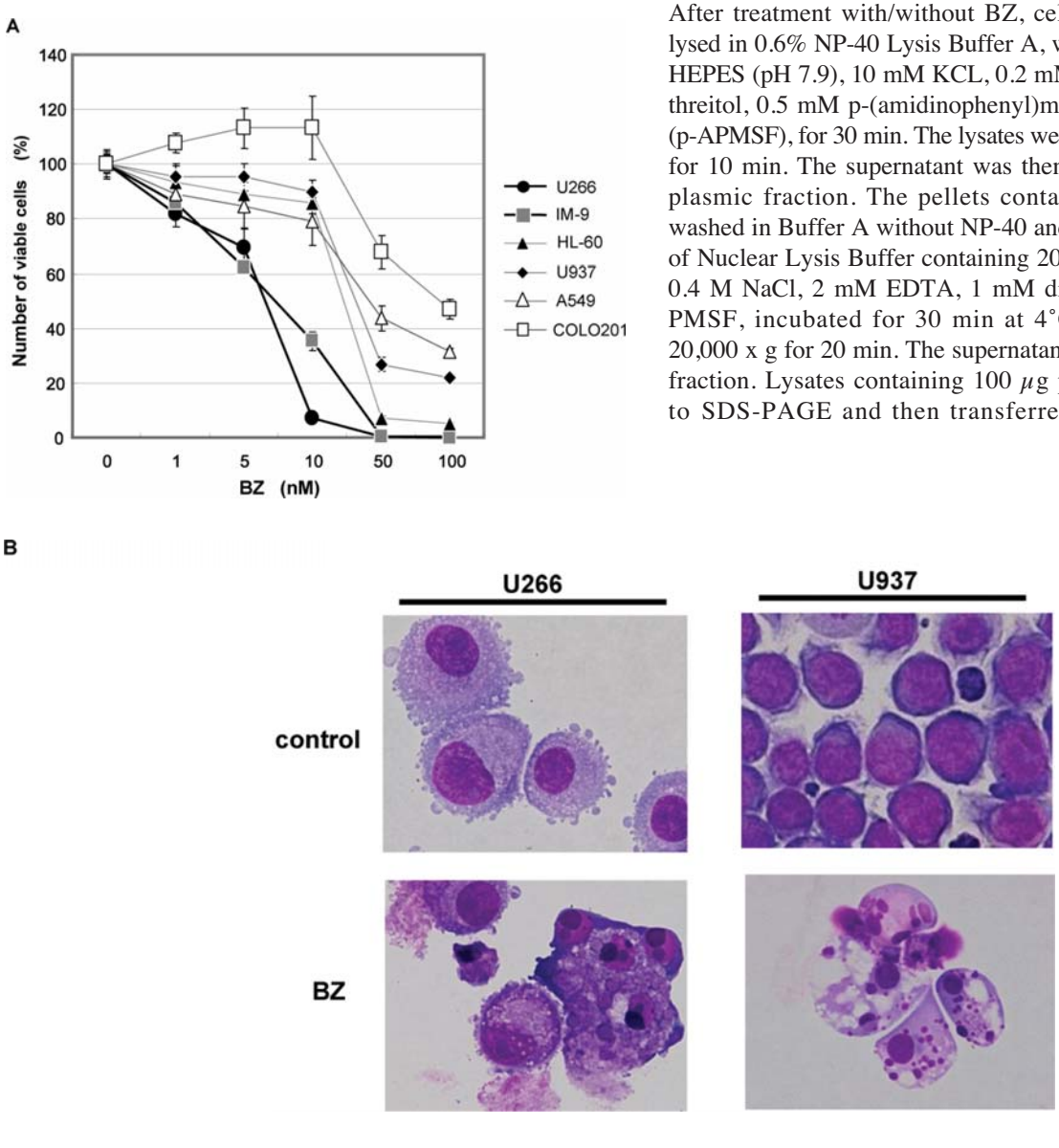

Figure 1. Cytotoxic effect of BZ in various cell lines. (A) Cell growth inhibition: cells were treated with BZ at various concentrations for 48 h. Viable cell number was assessed by CellTiter Blue as described in Materials and methods. (B) Morphological features after treatment with/without BZ (10 nM) for 24 h in U266 and U937 cells. May-Grünwald-Giemsa staining (original magnification, x1,000). (C) Immunoblotting with cleaved caspase-3: U266 cells were treated with BZ for 24 to 48 h. Cells were lysed, and cellular proteins were separated by 15% SDS-PAGE and immunoblotted with anti-cleaved caspase-3 Ab. Immunoblotting with anti-GAPDH mAb was performed as an internal control.

membrane (Millipore), and immunoblotted with primary antibodies (e.g., anti-NF-κB p65 Ab (Santa Cruz), anti-IκBα Ab, and anti-phospho-IκBα (Ser32/36) Ab (Cell Signaling).

Gene expression analysis. Total RNA was isolated from cell pellets using Isogen (Nippon Gene, Tokyo) and genomic DNA was removed using RQ1 RNase-Free DNase (Promega) at 37˚C for 30 min, followed by extraction with phenol chloroform and ethanol precipitation. Reverse-transcription using a PrimeScript RT Master Mix (Takara Bio Inc. Ohtsu, Japan) was performed according to the manufacturer's instructions. Real-time PCR was performed on 3 ng of cDNA using validated SYBR Green gene expression assays for human ATF6, IRE1, PERK, GRP78, ATF4, CHOP, GADD34, BIM, and BCL-2 in combination with SYBR Premix Ex Taq II (Takara Bio Inc.). All primers used in this study are listed in Table I. Quantitative real-time PCR was performed in duplicates in a Thermal Cycler Dice Real Time System TP800 (Takara Bio Inc.). The data were analyzed using Thermal Cycler Dice Real Time System Software (Takara Bio Inc.), and the comparative C_t method (2ΔΔCt) was used for relative quantification of gene expression. The data of real-time PCR products were standardized to GAPDH as an internal control. To confirm the specific amplification of target genes, each gene product after real-time PCR was further separated by 1.5% agarose gel to detect a single band at the theoretical product size, and the dissociation curves were analyzed to detect a single peak.

Transfection of LC3B siRNA. For the gene silence of LC3B in U266 cells, LC3B siRNA and a control scramble siRNA, whose sequences are described below, were diluted to a finial concentration of 20 nM in Opti-Mem I (Invitrogen, Paisley, UK), and transfection was performed with cells at 50% confluency using Oligofectamine transfection reagent (Invitrogen) according to the manufacturer's instruction. LC3B sense: CAAUCUCAGAGGUGUAUGTT; LC3B antisense: UCAUACACCUCUGAGAUUTT; control sense: GACUACUGGUCGUUGAACUTT; control antisense: AGUUCAACGACCAGUAGUCTT.

Tet-off system with atg5$^{-/-}$ mouse embryonic fibroblasts (MEFs). The m5-7 cell line, the *atg5* tet-off MEF system, was a kind gift from Dr Noboru Mizushima (Tokyo Medical and Dental University School of Health Science, Tokyo, Japan). Culture conditions for continuous maintenance and for knock-down of the *atg5* gene to inhibit autophagy was previously described in detail (21).

Statistical analysis. All data are given as the mean ± SD. Statistical analysis was performed by using Mann-Whitney's U test (two-tailed). The criterion for statistical significance was taken as $p<0.05$. To analyze synergism, the combination index (CI) for each treatment was determined using the method developed by Chou (22).

Results

BZ induces autophagy and apoptosis in MM cells. BZ inhibited cell growth in all cell lines tested in a dose-dependent manner (Fig. 1A). BZ has a more potent cytotoxic effect in MM cell lines, U266 and IM-9, than other leukemia/cancer cell lines. After 24 h-treatment with 10 nM BZ, U266 cells, as well as other leukemia cell lines, indicated chromatin condensation and fragmented nuclei, which are typical morphologic features of apoptosis. Cleaved caspase-3 was detected after treatment with BZ for 24 to 48 h, indicating that BZ induces apoptotic cell death (Fig. 1B and C).

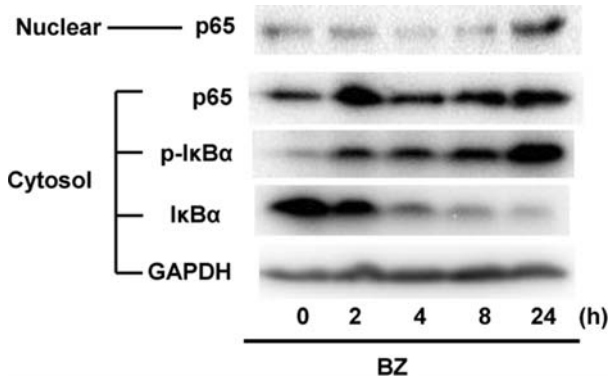

Figure 2. Intracellular distribution of NF-κB and IκBα after treatment with BZ in U266 cells. After treatment of U266 cells with BZ for 8 to 24 h, cytoplasmic and nuclear proteins were lysed and immunoblotting was performed using anti-NF-κB p65 Ab, anti-IκBα Ab, and anti-phospho-IκBα (Ser32/36) Ab. Immunoblotting with anti-GAPDH mAb was performed as an internal control.

In response to BZ, phosphorylation of IκBα along with a decreased level of cytoplasmic IκBα and increased nuclear NF-κB was observed (Fig. 2). This result suggests that BZ does not inhibit but rather activates the NF-κB pathway, as recently reported by others (23).

In addition to chromatin condensation and nuclear fragmentations, cytosolic debris and vacuoles were also observed in U266 cells (Fig. 1B). Electron microscopy revealed increased autophagosomes and autolysosomes after 24-h treatment with BZ (Fig. 3A). LC3 exists in two cellular forms, LC3-I and LC3-II. LC3-I is converted to LC3-II by conjugation to phosphatidylethanolamine during the formation of autophagosomes. Therefore, the amount of LC3-II is a good early marker for the formation of autophagosomes (24). Immunoblotting demonstrated that BZ treatment induced an increased ratio of LC3B-II to LC3B-I along with a reduction of p62 expression (Fig. 3B). All these data indicate that BZ induces autophagy, and the increased number of autophagosomes was not due to accumulation of autophagosomes by blocking autophagic flux (24). It is noteworthy that autophagy induction in response to BZ became prominent after 48-h exposure. In addition, basal LC3B-II conversion without BZ treatment appeared to be kept at a higher level in U266 cells than in other cell lines (Fig. 3B, upper panel).

To investigate whether autophagy induced by BZ has cytoprotective function or leads to cell death (i.e., autophagic cell death) and also whether inhibition of BZ-induced autophagy enhances ER stress-medicated apoptosis, we treated U266 cells with BZ in the presence or absence of 3-methyladenine (3-MA), an inhibitor of class III phosphatidylinositol-3 kinase (PI3K) for inhibiting autophagosome formation (25). Unexpectedly, cell growth inhibition in response to BZ was attenuated in the presence of 3-MA at

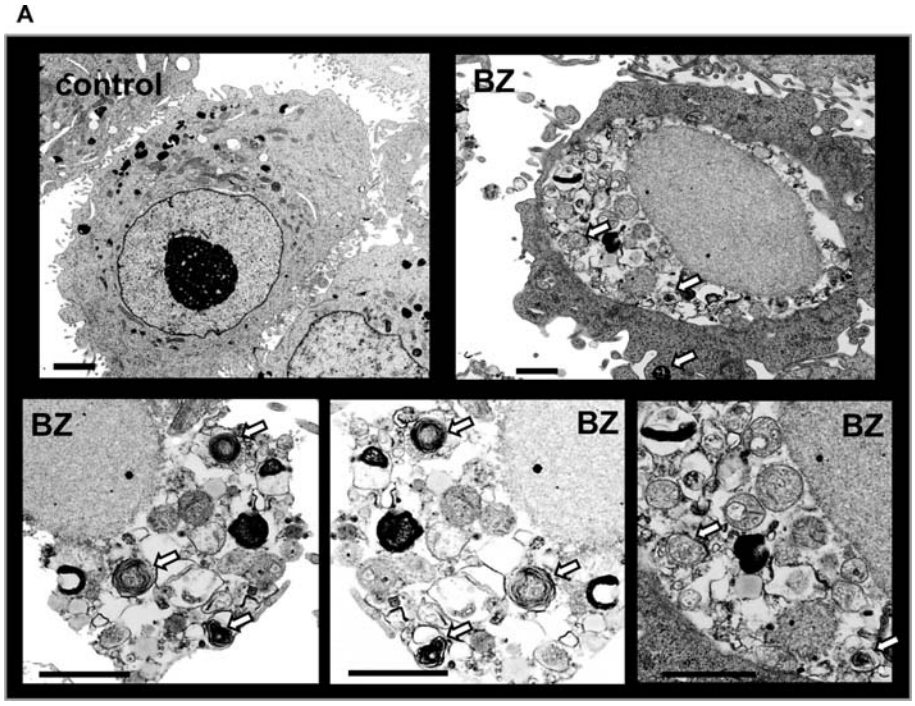

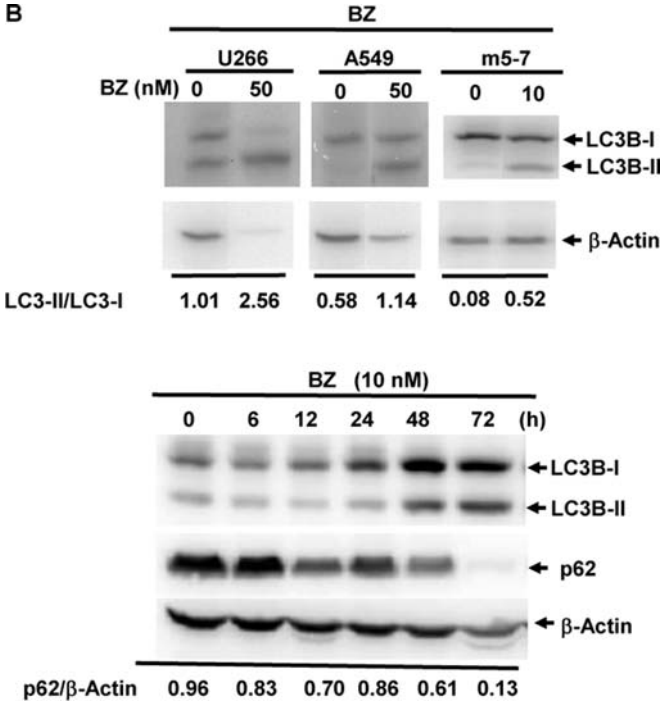

Figure 3. Autophagy induction after treatment with BZ. (A) Electron microscopy in U266 cells treated with/without BZ (10 nM) for 24 h. (B) Immunoblotting with anti-LC3B Ab and anti-p62 Ab. Upper panel: U266, A549 and m5-7 cells were treated with BZ at indicated concentrations for 48 h. Cellular proteins were separated by 15% SDS-PAGE and immunoblotted with anti-LC3B Ab. Lower panel: U266 cells were treated with BZ for various lengths of time. Cellular proteins were separated by 15% SDS-PAGE and immunoblotted with anti-LC3B Ab and anti-p62 Ab. Immunoblotting with anti-ß-actin mAb was performed as an internal control. Each number indicates the ratio of LC3B-II/LC3B-I and p62/ß-actin.

5 to 10 nM BZ (Fig. 4A). In addition, suppression of autophagy by siRNA mediated knockdown of LC3B in U266 cells as well as complete inhibition by knockout of *atg5* gene in the tet-off *atg5*$^{-/-}$ MEF system attenuated BZ-induced cytotoxicity (Fig. 4B and C). These data suggest that autophagy induction in response to BZ leads to cell death but not cytoprotection.

Combined treatment with BZ and bafilomycin A_1 synergizes cytotoxicity in U266 cells. Since treatment with 3-MA, siRNA for LC3B, and knockout of *atg5* gene all lead to suppression of early events of autophagosome formation, we next investigated the effect of bafilomycin A_1 (BAF). BAF is a strong selective inhibitor of vacuolar H(+)-ATPase (V-ATPase) *in vitro* and is used to inhibit autophagy at the late stage (26). Treatment with BAF alone resulted in weak cell growth inhibition at concentrations between 1 and 100 nM (Fig. 5A). However, combined treatment with BAF plus BZ synergistically enhanced cytotoxicity in U266 cells (Fig. 5B). The combination of MG-132, another proteasome inhibitor, with BAF resulted in pronounced cytotoxicity compared with cells treated with either MG-132 or BAF alone (data not shown). Cytotoxicity of BZ with/without BAF was weak with 24-h exposure, but became prominent after 48-h exposure (Fig. 5B).

BAF induces ER stress and JNK activation but with kinetics different from that by BZ-treatment. We next examined the change of expressions of ER stress-related genes including ATF6, PERK and IRE1, and their downstream molecules [e.g., GRP78 (Bip), CHOP (GADD153), and BCL-2] after treatment with either BZ and/or BAF in U266 cells. GADD34 was up-regulated whereas BCL-2 was down-regulated after treatment with BZ, but not with BAF. Prominent amplifications of GRP78 and CHOP mRNAs were observed after treatment with BZ and/or BAF (Table II). However, the kinetics of CHOP/GRP78 were completely different between BZ- and BAF-treatments. GRP78 and CHOP were induced within 8 h after treatment with BZ and a peak level was detected at 24 h-exposure. This gene profile appears to be similar to that produced by tunicamycin, a well-known potent

ER stress inducer that blocks the synthesis of all N-linked glycoproteins (N-glycans) (Fig. 6A). In contrast, BAF induced GRP78/CHOP after more than 24 h-exposure. Induction of GRP78 and CHOP mRNAs was rather pronounced after 48-h treatment with BAF, compared with that induced by BZ. Phosphorylation of JNK (Thr183/Tyr185) was detected in response to either BZ or BAF treatment (Fig. 6B). Kinetics of pro-apoptotic JNK activation matched well with those of CHOP/GRP78 induction. Interestingly, combined treatment with BZ and BAF resulted in an ER stress pattern similar to that with BZ treatment. JNK activation at 36 h appears to be enhanced, compared with either BZ or BAF alone. PERK kinase mediates the initial stress response by phosphorylation of the α subunit of the eukaryotic initiation factor 2 (eIF2) to attenuate protein synthesis (9,18). Phosphorylation of eIF2α

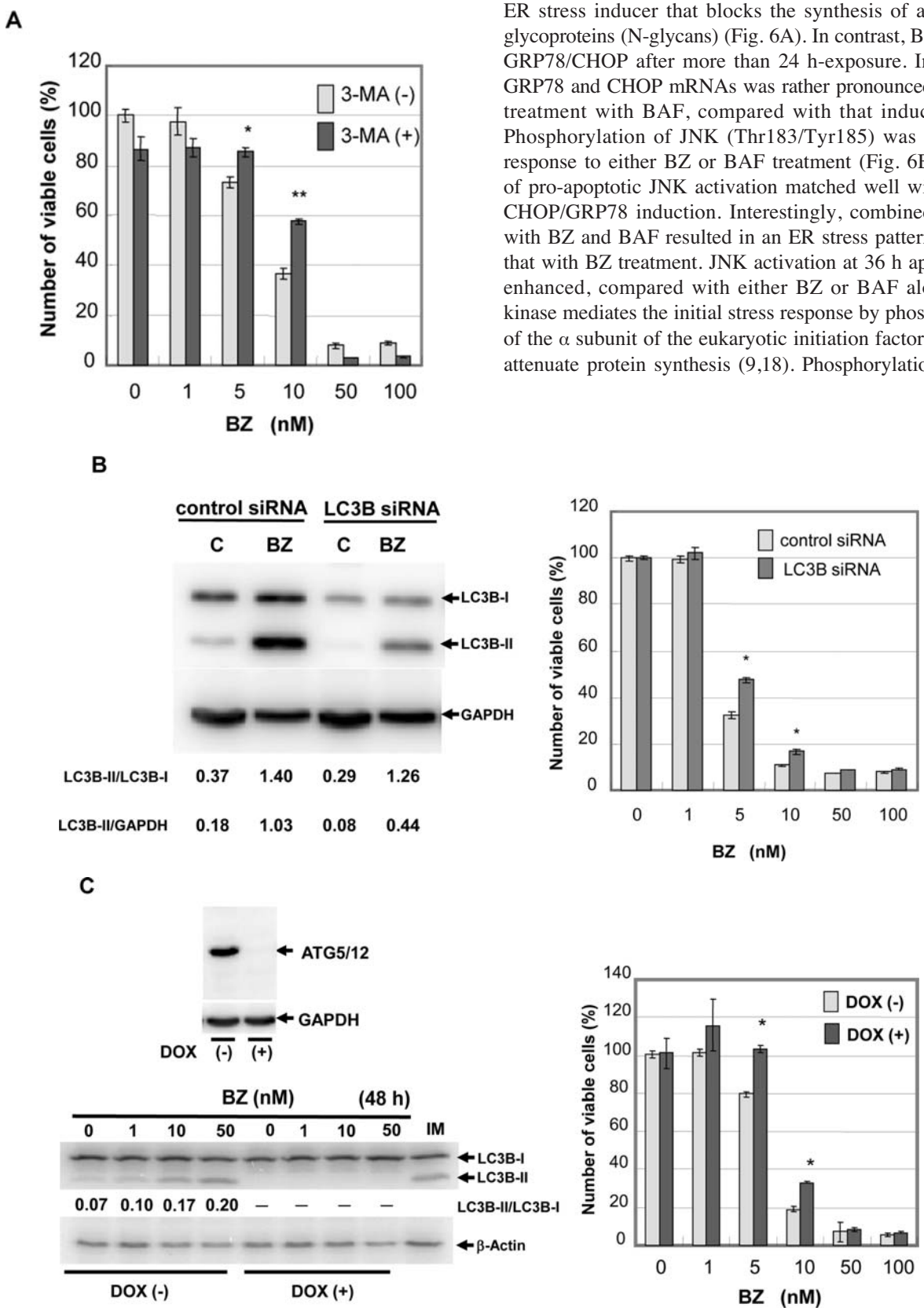

Figure 4. Effect of 3-MA, siRNA for LC3B, and *atg*5 knockdown in BZ-induced cytotoxicity. (A) U266 cells were cultured with BZ at various concentrations in the presence or absence of 1 mM of 3-MA for 48 h. The viable cell number was assessed as described in Materials and methods ($^{*}p<0.005$, $^{**}p<0.001$: 3-MA treated vs. 3-MA untreated). (B) U266 cells were pretreated with either siRNA for LC3B or control scramble siRNA for 48 h and subsequently treated with BZ for 48 h. Viable cell number was assessed ($^{*}p<0.001$: siRNA for LC3B vs. scramble siRNA). In addition, cellular proteins were lysed and immunoblotted with anti-LC3B Ab. Immunoblotting with anti-GAPDH mAb was performed as an internal control. Each number indicates the ratio of LC3B-II/LC3B-I and LC3B-II/GAPDH. (C) Tet-off atg5 m5-7 cells: m5-7 cells were pretreated with/without 10 ng/ml doxycycline (Dox) for 96 h for knockdown of *atg5*. Thereafter, cells were cultured with BZ at various concentrations for 48 h, viable cell number was assessed ($^{*}p<0.001$: Dox treated vs. Dox untreated cells). Cellular proteins were lysed and immunoblotted with either anti-LC3B Ab or anti-ATG5 Ab. Cell lysate from Dox (-) m5-7 cells treated with an autophagy inducer imatinib mesylate (IM, 10 μM) for 48 h was used as a positive control for detecting LC3B-II. Immunoblotting with either anti-GAPDH mAb or anti-ß-actin mAb was performed as an internal control. Each number indicates the ratio of LC3B-II/LC3B-I.

in response to BAF was detected at 24 h and persisted during 48-h exposure, while no eIF2α phosphorylation was detectable during 48 h-treatment with BZ alone (Fig. 6B). With combined treatment using BZ plus BAF, almost no eIF2α phosphorylation was detected. All these data demonstrate that BAF, a late stage autophagy inhibitor, induces ER stress as well as BZ. However, the quality of ER stress including kinetics appears to differ between these two reagents.

Sequential exposure to BAF and BZ induces potent cytotoxicity in U266 cells. The profile of ER stress induction in response to BZ and BAF suggests that BAF-treatment requires more time for loading ER stress for inducing pro-apoptotic CHOP and JNK phosphorylation. To synchronize ER stress for optimal induction for ER stress-based cytotoxicity, we next attempted sequential exposure to BAF and BZ. U266 cells were pretreated with 10 nM of BAF for 48 h; then BAF was washed out; and subsequent treatment was performed with various concentrations of BZ for 48 h. Pre-treatment with BAF enhanced BZ-induced cytotoxicity, compared with that in U266 cells without pre-treatment with BAF (Fig. 7). In addition, cytotoxicity was more pronounced than with simultaneous combination of BAF and BZ for 48 h.

Discussion

In the present study we demonstrated that a proteasome inhibitor, BZ induces autophagy as well as ER stress in MM cells (Fig. 3 and Table II). In addition, an autophagy inhibitor, BAF also induces ER stress along with upregulation of pro-apoptotic CHOP expression (Table II and Fig. 6A). The direct linkage was demonstrated between the autophagy-lysosome system and the ubiquitin-proteasome system via p62 docking protein (14,15). On the other hand, accumulating data now indicate that ER stress is a potent trigger of autophagy (27). Potent ER-stress inducers such as tunicamycin (an inhibitor of N-glycosylation) and thapsigargin (an inhibitor of ER Ca^{2+}-ATPase), induce autophagy (16). In these cases, ER-stress-induced autophagy counterbalances the ER expansion, removes aggregated proteins from ER, and serves a cytoprotective function. Recent reports demonstrated that BZ treatment induced autophagy in the breast cancer MCF-7 cells by a mechanism that involved proteasomal stabilization of ATF4 and ATF4-dependent upregulation of LC3B (28). ATF4, which is a transcription factor and a component of the PERK pathway, facilitated

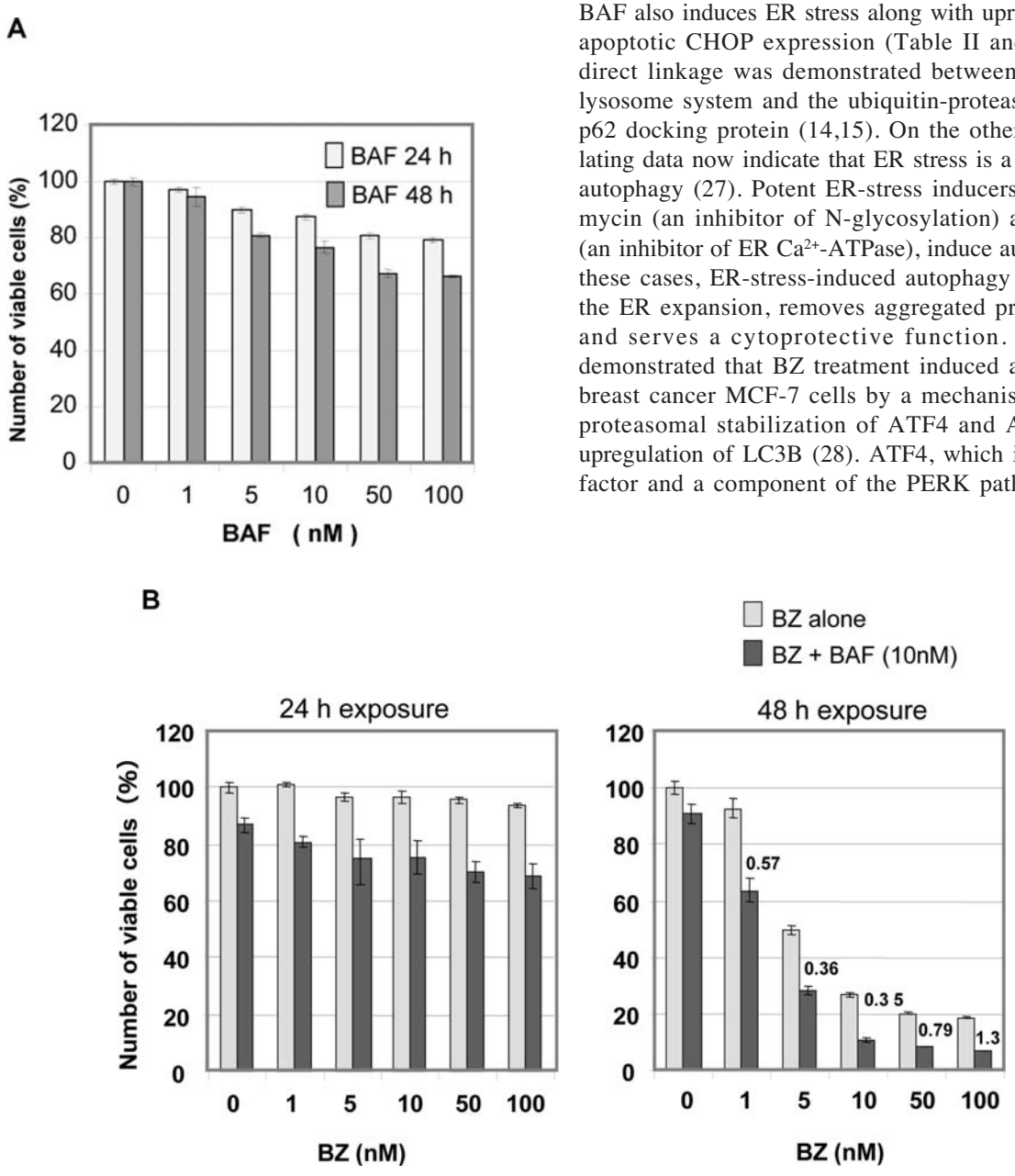

Figure 5. Cytotoxic effect after combined treatment with BZ plus BAF in U266 cells. (A) Cells were cultured with BAF at various concentrations for 24 and 48 h. Viable cell number was assessed as described in Materials and methods. (B) Cells were cultured with BZ at various concentrations for 24 and 48 h in the presence or absence of BAF (10 nM). Each number indicates CI. CI<1 indicates the synergistic effect produced by combined treatment with BZ and BAF (22).

Table II. Profiles of ER stress related genes after treatment with BZ and/or BAF in U266 cells.

Symbol	Tx	8 h Fold change (± SD)	24 h Fold change (± SD)	48 h Fold change (± SD)
ATF6	BZ	1.04 (±0.04)	1.17 (±0.03)	0.63 (±0.03)
	BAF	1.16 (±0.06)	0.71 (±0.03)	1.44 (±0.07)
	BZ + BAF	1.47 (±0.09)	1.24 (±0.07)	0.69 (±0.05)
PERK	BZ	0.85 (±0.04)	0.81 (±0.06)	0.23 (±0.03)
	BAF	1.65 (±0.02)	1.29 (±0.09)	4.91 (±0.21)
	BZ + BAF	1.28 (±0.13)	0.89 (±0.06)	0.29 (±0.01)
IRE1	BZ	3.27 (±0.12)	2.52 (±0.19)	0.82 (±0.07)
	BAF	1.41 (±0.11)	0.65 (±0.10)	1.75 (±0.15)
	BZ + BAF	4.33 (±0.14)	2.96 (±0.16)	0.87 (±0.18)
GRP78	BZ	2.29 (±0.21)	3.97 (±0.15)	2.96 (±0.27)
	BAF	1.25 (±0.06)	0.63 (±0.06)	9.19 (±0.51)
	BZ + BAF	2.28 (±0.37)	5.32 (±0.55)	2.82 (±0.17)
ATF4	BZ	2.35 (±0.05)	1.75 (±0.08)	2.14 (±0.09)
	BAF	1.66 (±0.07)	0.98 (±0.15)	2.51 (±0.07)
	BZ + BAF	3.05 (±0.26)	2.20 (±0.11)	2.40 (±0.09)
CHOP	BZ	4.98 (±0.39)	6.48 (±0.35)	5.48 (±0.32)
	BAF	2.20 (±1.30)	1.60 (±0.06)	32.56 (±4.25)
	BZ + BAF	5.58 (±0.11)	6.70 (±0.13)	4.47 (±0.23)
GADD34	BZ	3.28 (±0.15)	8.11 (±0.15)	9.99 (±0.47)
	BAF	1.35 (±0.15)	1.26 (±0.03)	1.38 (±0.56)
	BZ + BAF	3.69 (±0.19)	9.58 (±0.19)	8.82 (±0.70)
BIM	BZ	1.28 (±0.11)	0.99 (±0.03)	0.58 (±0.02)
	BAF	0.99 (±0.01)	0.89 (±0.08)	1.04 (±0.11)
	BZ + BAF	1.16 (±0.05)	1.25 (±0.10)	0.60 (±0.15)
BCL-2	BZ	0.34 (±0.03)	0.17 (±0.08)	0.07 (±0.07)
	BAF	2.23 (±0.48)	1.19 (±0.31)	0.99 (±0.04)
	BZ + BAF	0.73 (±0.23)	0.19 (±0.01)	0.09 (±0.01)

U266 cells were treated with either BZ (10 nM) and/or BAF (10 nM) for indicated time period. Gene expression was analyzed by real-time PCR as described in Materials and methods. Expression level was compared with that in untreated control cells. Mean (± SD).

autophagy through direct binding to a cyclic AMP response element binding site in the LC3B promoter, following upregulation of LC3B and autophagy induction in response to sever hypoxia (29). Therefore, crosstalk among the ubiquitin-proteasome system, the autophagy-lysosome system, and ER stress was suggested (Fig. 8). Based on this proposed model, we hypothesized that combined treatment with BZ and an autophagy inhibitor enhances ER-stress medicated cytotoxicity in MM cells.

Against our initial expectation, combinations of BZ with either 3-MA or siRNA for LC3B attenuated BZ-induced cytotoxicity (Fig. 4A and B). Furthermore, the complete knockdown of *atg5* gene in the tet-off MEF system indicated the suppression of BZ-induced cell death (Fig. 4C). These data suggest that autophagy induction in response to BZ leads to cell death, but not cytoprotective or cell adaptation. Similar results have been reported by others, demonstrating that combined treatment with BZ and either 3-MA or siRNA for *beclin-1* resulted in antagonistic response (30). However, we still detected synergistic enhancement in cytotoxicity with a combination of BZ and BAF (Fig. 5). We cannot yet fully explain this discrepancy. BAF is a macrolide antibiotic that was initially characterized for its selective inhibition of V-ATPase (31). At nanomole concentrations, BAF disrupts the vesicular proton gradients and ultimately increases the pH of acidic vesicles (31). This disruption of vesicular acidification by BAF prevents the fusion of autophagosomes with lysosomes, resulting in inhibition of autophagy (31,32). Therefore, the completely opposite behavior in BZ-induced cytotoxicity by combination with either 3-MA treatment or LC3B siRNA, which are all involved in inhibiting initial autophagosome formation, and with BAF working to inhibit fusion of

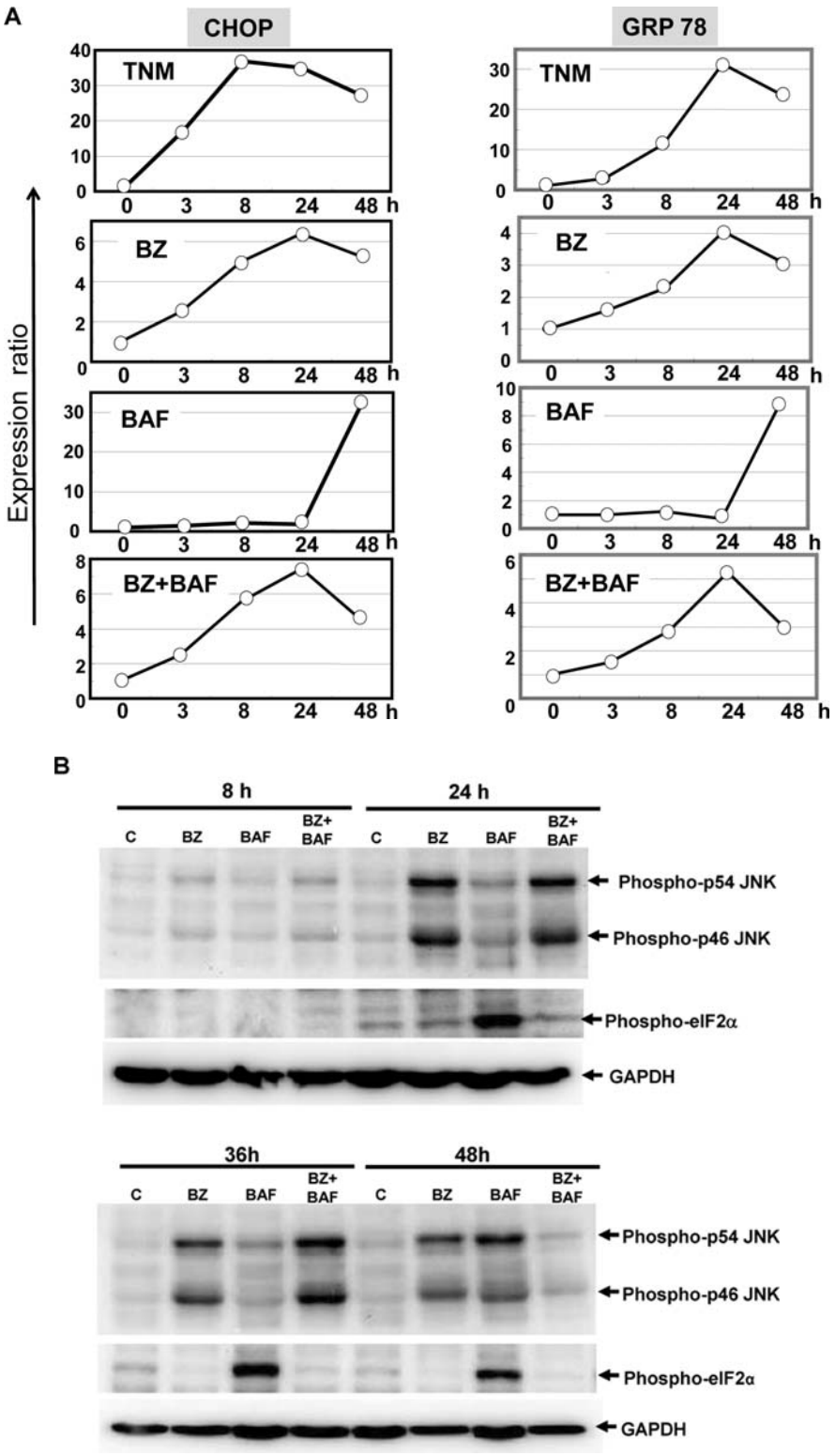

Figure 6. ER stress induction in response to either BZ and/or BAF in U266 cells. (A) Kinetics of GRP78 and CHOP expressions assessed by quantitative real-time PCR during exposure to 10 nM BZ, 10 nM BAF, 10 nM BZ plus 10 nM BAF. Tunicamycin (TNM: 1 μg/ml) was used as an ER stress inducer. (B) Phosphorylation of eIF2α and JNK after treatment with BZ and/or BAF in U266 cells. After treatment with BZ (10 nM) for 8 to 48 h, cellular proteins were lysed, separated by 11.25% SDS-PAGE, and immunoblotted with either anti-phospho-JNK (Thr183/Tyr185) Ab or anti-phospho-eIF2α (Ser51) Ab. Immunoblotting with anti-GAPDH mAb was performed as an internal control.

autophagosome and lysosome, might be due to the different inhibition of the stage of the autophagic process. It has been reported that imatinib mesylate, an inhibitor of tyrosine kinase, induced cytotoxicity associated with autophagy in malignant glioma cells. Also, imatinib-induced cytotoxicity was attenuated by inhibiting autophagy at an early stage by 3-MA,

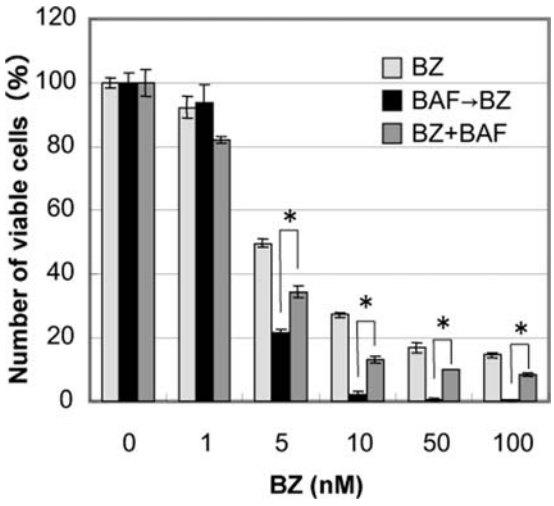

Figure 7. Cytotoxic effect after sequential exposure to BAF and BZ in U266 cells. After 48 h pre-treatment of U266 cells with 10 nM BAF, cells were washed and subsequently treated with BZ at various concentrations for 48 h. Numbers of viable cells were compared with those in cells without pre-treatment with BAF and in cells simultaneously treated with BZ and BAF (10 nM) for 48 h ($^*p<0.001$: BAF→BZ vs. BZ+BAF).

while inhibiting autophagy at a late stage by BAF augmented cytotoxicity through increasing apoptosis (33). Not shown is that complete knockdown of *atg5* gene in m5-7 cells resulted in no enhancement of CHOP induction. A recent report demonstrated atg5/atg7-independent autophagosome formation (34). Therefore, an alternative pathway for autophagosome formation might be involved.

Although the precise biological significance of the stage-specific inhibition of autophagy for modulating cytotoxicity remains unknown we have demonstrated that BAF treatment induces ER stress, as well as pro-apoptotic CHOP and other ER stress markers. However, a difference in the quality of ER stress was observed between BZ- and BAF-treatment. First, BZ at 10 nM induced a series of ER stress markers within 8 h, whereas BAF required 48-h exposure (Table II and Fig. 6A). This may be because autophagy-lysosomal protein degradation appears to locate in a more distal site than proteasomal protein degradation during accumulating ER stress. Inversely, BZ appears to require more time to induce autophagy than other potent autophagy inducers (Fig. 3B) (35). Second, as indicated in Fig. 6B, phosphorylation of eIF2α by BAF was detected at 24 h and persisted during 48-h exposure, whereas no eIF2α phosphorylation was detectable during 48-h treatment with BZ alone. It was reported that MM cells surviving BZ-treatment attenuated both eIF2α phosphorylation and CHOP induction (36). Therefore, combined treatment with salubrinal, which inhibits GADD34-protein phosphatase 1 (PPI) complex, restored eIF2α phosphorylation and CHOP induction, maximizing BZ-induced apoptosis. Thus, strategies capable of sustaining CHOP expression appear to be required for successful eradication of MM cells (36).

Proteasome inhibitor BZ has been thought to inhibit NF-κB in MM cells via inhibiting ubiquitinated IκBα degradation (4-6). However, the intracellular distribution of NF-κB and IκBα as well as the phosphorylation state of IκBα, suggests that NF-κB is rather activated in response to BZ in U266 cells (Fig. 2). This result is also supported by a recent report by Hideshima and colleagues, who demonstrated that BZ activated a canonical NF-κB pathway in MM cell lines and primary cultured MM cells *in vitro* (23). Therefore, other molecular-based mechanism(s) leading to cell death, including ER stress, appears to contribute to the

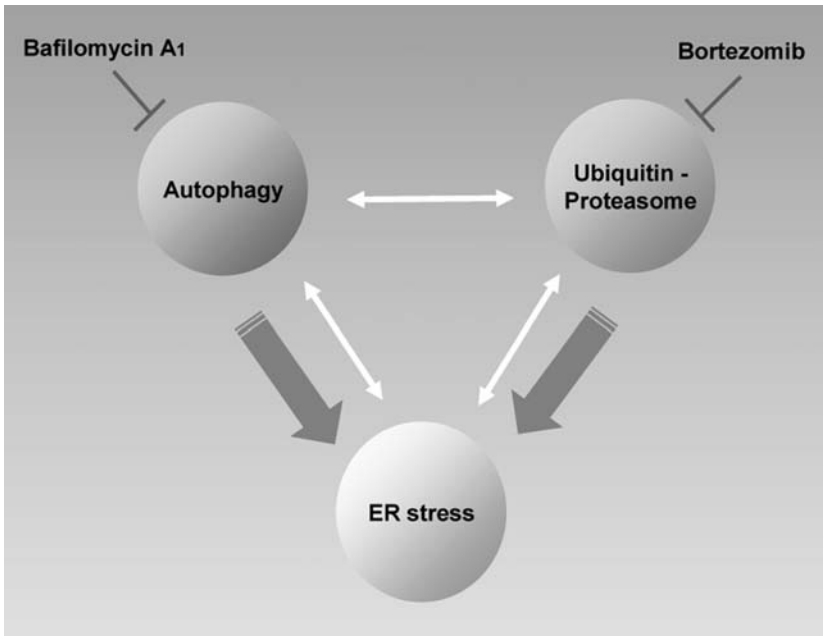

Figure 8. Proposed model for crosstalk among the ubiquitin-proteasome system, the autophagy-lysosome system, and ER stress.

therapeutic effect of BZ for MM. Previous reports demonstrated that NF-κB promoted cell survival during ER stress by repressing CHOP expression (37,38). The p65 subunit but not p50 subunit of NF-κB was reported to repress CHOP promoter activity (37). Therefore, repression rather than enhancement of CHOP expression by combined treatment with BZ plus BAF for 48 h may be due to NF-κB activation in response to BZ. It has been reported that combined treatment with BZ and NF-κB inhibitor enhances the cytocidal effect in MM cells by an unknown mechanism (23). Based on our results indicating the difference in kinetics of ER stress between BZ and BAF, we attempted to synchronize ER stress by sequential exposure to BAF followed by BZ to maximize and sustain ER stress, including CHOP induction. This further enhances cytotoxicity in U266 cells (Fig. 7). Therefore, controlling the kinetics of the relation among autophagy, proteasome and ER stress appears to have important implications for optimizing cancer treatment, including MM-therapy.

Acknowledgements

We thank Dr Noboru Mizushima (Tokyo Medical and Dental University School of Health Science, Tokyo, Japan) for the kind gift of a tet-off *atg5* m5-7 cell line. This study is supported in part by a Grant-in-Aid for Scientific Research (C) from the Ministry of Education, Culture, Sports, Science and Technology of Japan to K.M. (no. 22591050), funds from the Private University Strategic Research-Based Support Project (Molecular Information-based Intractable Disease Research Project) from the Ministry of Education, Culture, Sports, Science and Technology of Japan to A.T. and K.M. (2008-2012), and a grant from the Tokyo Medical University Cancer Research Foundation to K.M.

References

1. Shah JJ and Orlowski RZ: Proteasome inhibitors in the treatment of multiple myeloma. Leukemia 23: 1964-1979, 2009.
2. San Miguel JF, Schlag R, Khuageva NK, Dimopoulos MA, Shpilberg O, Kropff M, Spicka I, Petrucci MT, Palumbo A, Samoilova OS, Dmoszynska A, Abdulkadyrov KM, Schots R, Jiang B, Mateos MV, Anderson KC, Esseltine DL, Liu K, Cakana A, van de Velde H and Richardson PG: VISTA Trial Investigators. Bortezomib plus melphalan and prednisone for initial treatment of multiple myeloma. N Engl J Med 359: 906-917, 2008.
3. Adams J: The proteasome: a suitable antineoplastic target. Nat Rev Cancer 4: 349-360, 2004.
4. Mitsiades N, Mitsiades CS, Poulaki V, Chauhan D, Fanourakis G, Gu X, Bailey C, Joseph M, Libermann TA, Treon SP, Munshi NC, Richardson PG, Hideshima T and Anderson KC: Molecular sequelae of proteasome inhibition in human multiple myeloma cells. Proc Natl Acad Sci USA 99: 14374-14379, 2002.
5. Hideshima T, Chauhan D, Richardson P, Mitsiades C, Mitsiades N, Hayashi T, Munshi N, Dang L, Castro A, Palombella V, Adams J and Anderson KC: NF-kappa B as a therapeutic target in multiple myeloma. J Biol Chem 277: 16639-16647, 2002.
6. Berenson JR, Ma HM and Vescio R: The role of nuclear factor-kappaB in the biology and treatment of multiple myeloma. Semin Oncol 28: 626-633, 2001.
7. Meister S, Schubert U, Neubert K, Herrmann K, Burger R, Gramatzki M, Hahn S, Schreiber S, Wilhelm S, Herrmann M, Jäck HM and Voll RE: Extensive immunoglobulin production sensitizes myeloma cells for proteasome inhibition. Cancer Res 67: 1783-1792, 2007.
8. Obeng EA, Carlson LM, Gutman DM, Harrington WJ Jr, Lee KP and Boise LH: Proteasome inhibitors induce a terminal unfolded protein response in multiple myeloma cells. Blood 107: 4907-4916, 2006.
9. Ron D and Walter P: Signal integration in the endoplasmic reticu-lum unfolded protein response. Nat Rev Mol Cell Biol 8: 519-529, 2007.
10. Moretti L, Cha YI, Niermann KJ and Lu B: Switch between apoptosis and autophagy: radiation-induced endoplasmic reticulum stress? Cell Cycle 6: 793-798, 2007.
11. Levine B and Kroemer G: Autophagy in the pathogenesis of disease. Cell 132: 27-42, 2008.
12. Mizushima N, Levine B, Cuervo AM and Klionsky DJ: Autophagy fights disease through cellular self-digestion. Nature 451: 1069-1075, 2008.
13. Kirkin V, McEwan DG, Novak I and Dikic I: A role for ubiquitin in selective autophagy. Mol Cell 34: 259-269, 2009.
14. Moscat J and Diaz-Meco MT: p62 at the crossroads of autophagy, apoptosis, and cancer. Cell 137: 1001-1004, 2009.
15. Komatsu M and Ichimura Y: Physiological significance of selective degradation of p62 by autophagy. FEBS Lett 584: 1374-1378, 2010.
16. Ding WX, Ni HM, Gao W, Hou YF, Melan MA, Chen X, Stolz DB, Shao ZM and Yin XM: Differential effects of endoplasmic reticulum stress-induced autophagy on cell survival. J Biol Chem 282: 4702-4710, 2007.
17. Yorimitsu T and Klionsky DJ: Endoplasmic reticulum stress: a new pathway to induce autophagy. Autophagy 3: 160-162, 2007.
18. Verfaillie T, Salazar M, Velasco G and Agostinis P: Linking ER stress to autophagy: potential implications for cancer therapy. Int J Cell Biol 2010: 1-19, 2010.
19. Yokoyama T, Miyazawa K, Naito M, Toyotake J, Tauchi T, Itoh M, Yuo A, Hayashi Y, Georgescu MM, Kondo Y, Kondo S and Ohyashiki K: Vitamin K2 induces autophagy and apoptosis simultaneously in leukemia cells. Autophagy 4: 629-640, 2008.
20. Zheng CL, Che XF, Akiyama S, Miyazawa K and Tomoda A: 2-Aminophenoxazine-3-one induces cellular apoptosis by causing rapid intracellular acidification and generating reactive oxygen species in human lung adenocarcinoma cells. Int J Oncol 36: 641-650, 2010.
21. Hosokawa N, Hara Y and Mizushima N: Generation of cell lines with tetracycline-regulated autophagy and a role for autophagy in controlling cell size. FEBS Lett 581: 2623-2629, 2007.
22. Chou TC: Theoretical basis, experimental design, and computerized simulation of synergism and antagonism in drug combination studies. Pharmacol Rev 58: 3621-3681, 2006.
23. Hideshima T, Ikeda H, Chauhan D, Okawa Y, Raje N, Podar K, Mitsiades C, Munshi NC, Richardson PG, Carrasco RD and Anderson KC: Bortezomib induces canonical nuclear factor-kappaB activation in multiple myeloma cells. Blood 114: 1046-1052, 2009.
24. Mizushima N and Yoshimori T: How to interpret LC3 immunoblotting. Autophagy 3: 542-545, 2007.
25. Seglen PO and Gordon PB: 3-Methyladenine: specific inhibitor of autophagic/lysosomal protein degradation in isolated rat hepatocytes. Proc Natl Acad Sci USA 79: 1889-1892, 1982.
26. Yoshimori T, Yamamoto A, Moriyama Y, Futai M and Tashiro Y: Bafilomycin A1, a specific inhibitor of vacuolar-type H(+)-ATPase, inhibits acidification and protein degradation in lysosomes of cultured cells. J Biol Chem 266: 17707-17712, 1991.
27. Høyer-Hansen M and Jäättelä M: Connecting endoplasmic reticulum stress to autophagy by unfolded protein response and calcium. Cell Death Differ 14: 1576-1582, 2007.
28. Milani M, Rzymski T, Mellor HR, Pike L, Bottini A, Generali D and Harris AL: The role of ATF4 stabilization and autophagy in resistance of breast cancer cells treated with bortezomib. Cancer Res 69: 4415-4423, 2009.
29. Rzymski T, Milani M, Pike L, Buffa F, Mellor HR, Winchester L, Pires I, Hammond E, Ragoussis I and Harris AL: Regulation of autophagy by ATF4 in response to severe hypoxia. Oncogene 29: 4424-4435, 2010.
30. Hoang B, Benavides A, Shi Y, Frost P and Lichtenstein A: Effect of autophagy on multiple myeloma cell viability. Mol Cancer Ther 8: 1974-1984, 2009.
31. Yamamoto A, Tagawa Y, Yoshimori T, Moriyama Y, Masaki R and Tashiro Y: Bafilomycin A_1 prevents maturation of autophagic vacuoles by inhibiting fusion between autophagosomes and lysosomes in rat hepatoma cell line, H-4-II-E cells. Cell Struct Funct 23: 33-42, 1998.

32. Shacka JJ, Klocke BJ, Shibata M, Uchiyama Y, Datta G, Schmidt RE and Roth KA: Bafilomycin A1 inhibits chloroquine-induced death of cerebellar granule neurons. Mol Pharmacol 69: 1125-1136, 2006.
33. Shingu T, Fujiwara K, Bögler O, Akiyama Y, Moritake K, Shinojima N, Tamada Y, Yokoyama T and Kondo S: Stage-specific effect of inhibition of autophagy on chemotherapy-induced cytotoxicity. Autophagy 5: 537-539, 2009.
34. Nishida Y, Arakawa S, Fujitani K, Yamaguchi H, Mizuta T, Kanaseki T, Komatsu M, Otsu K, Tsujimoto Y and Shimizu S: Discovery of Atg5/Atg7-independent alternative macroautophagy. Nature 461: 654-658, 2009.
35. Ohtomo T, Miyazawa K, Naito M, Moriya S, Kuroda M, Itoh M and Tomoda A: Cytoprotective effect of imatinib mesylate in non-BCR-ABL-expressing cells along with autophagosome formation. Biochem Biophys Res Commun 391: 310-315, 2010.
36. Schewe DM and Aguirre-Ghiso JA: Inhibition of eIF2alpha dephosphorylation maximizes bortezomib efficiency and eliminates quiescent multiple myeloma cells surviving proteasome inhibitor therapy. Cancer Res 69: 1545-1552, 2009.
37. Nozaki S, Sledge GW Jr and Nakshatri H: Repression of GADD153/CHOP by NF-kappaB: a possible cellular defense against endoplasmic reticulum stress-induced cell death. Oncogene 20: 2178-2185, 2001.
38. Schapansky J, Olson K, Van Der Ploeg R and Glazner G: NF-kappaB activated by ER calcium release inhibits Abeta-mediated expression of CHOP protein: enhancement by AD-linked mutant presenilin 1. Exp Neurol 208: 169-176, 2007.